Photoluminescence and optical properties of CuO thin films deposited via spray pyrolysis: influence of substrate temperature

Hassan Zare Asl[1,*] iD, Seyed Mohammad Rozati[2] iD

[1]*Department of Physics, Behbahan Khatam Alanbia University of Technology, Behbahan, Iran.*
[2]*Department of Physics, University of Guilan, Rasht, Iran.*

*****Corresponding author:** Zare@bkatu.ac.ir

Abstract:

CuO thin films were spray-deposited onto a glass substrate and the deposition temperature was varied from 450 to 550° C with 25° C steps. The 450° C deposition temperature was found to be the optimum condition for crystal growth. However, the FESEM images revealed that the grain size increases with raising the deposition temperature. To investigate the optical properties, the transmittance and reflectance data of the resulting films were recorded, and their optical constants, including absorption coefficient, band gap, Urbach energy, refractive index, extinction coefficient, and real and imaginary parts of the dielectric constant were calculated. All the prepared CuO thin films exhibited band gap values around 2.00 eV, which slightly declined with increasing the substrate temperature. The general trend of real and imaginary parts of the dielectric constant was increment and decrement, respectively, with increasing the substrate temperature. The spray-deposited CuO thin films were also excited at 486 nm, and the resulting photoluminescence (PL) spectra were recorded at room temperature. Three main and three shoulder peak emissions were detected in the recorded PL of all CuO thin films. The lowest peak intensity was related to the CuO thin film deposited at 500° C.

1. Introduction

Cupric oxide (CuO) is an intrinsically weak p-type semiconductor with a monoclinic structure [1]. Depending on the method and production parameters, a relatively wide range of optical band gaps ($1.3 - 2.1$ eV) has been reported in the literature [2]. However, characteristics such as thermal stability, nontoxicity, low production cost, and having a band gap close to the optimum band gap for the invisible light absorption make CuO an interesting choice for many technological applications [3]. Thus, CuO has been used in numerous electronic and optoelectronic devices such as solar cells [4], diodes [5], photoelectrochemical cells [6], thin-film transistors [7], gas sensors [8], photocatalysts [9], and cross-point memories [10].

The most commonly used form of the CuO nanostructure is its thin film that can be deposited via almost all conventional methods, including sputtering [11], electrodeposition [12], thermal oxidation [13], SILAR [14], sol-gel [15], and spray pyrolysis [16]. Among the aforementioned methods, spray pyrolysis is a solution-based and non-vacuum technique that provides cost-effectiveness and facility [17]. There are numerous studies examining the influence of spray-deposition parameters (substrate temperature [18], solution properties [19, 20], nozzle-substrate distance [21], and solution flow rate [22]) on the properties of the resulting film. Based on these studies, a relatively wide range of characteristics can be obtained for CuO thin films by adjusting the deposition parameters.

Considering the potential use of CuO thin films in optoelectronic devices, it is essential to study the optical properties of CuO thin films. However, to the best of our knowledge, there are few studies thoroughly investigating the optical properties of CuO thin films. Most relevant studies have

Table 1. Measured thickness, calculated texture coefficient, and structural parameters for the spray-deposited CuO thin films at different substrate temperatures.

Substrate Temperature	Thickness	Texture Coefficient		Crystallite Size		Lattice Parameter				
T	t	(002)	(111)	(002)	(111)	a (Å)	b (Å)	c (Å)	β (°)	V (Å^3)
(°C)	(nm)			(nm)	(nm)					
450	265	0.449	0.516	16	11	4.648	3.401	5.070	99.361	79.087
475	275	0.824	0.900	13	11	4.570	3.401	5.043	99.218	77.370
500	310	0.930	1.022	12	11	4.647	3.389	5.066	99.392	78.711
525	245	0.784	0.734	12	10	4.650	3.400	5.075	99.849	79.053
550	230	0.842	0.823	11	10	4.585	3.389	5.049	99.135	77.471

only reported experimental transmittance, reflectance, and estimation of the optical band gap. Yahia et al. [23], for instance, employed the spin coating sol-gel technique to grow a CuO film with nanorod morphology and calculate its optical constants. Furthermore, few studies have reported the photoluminescence (PL) characteristics of CuO thin films. Xu et al. [24] used the sol-gel method to deposit CuO thin films on a glass substrate. They studied the influence of film thickness on band gap variation and PL emission of the prepared films. Gobbiner et al. [25] also explored the influence of thickness on the PL characteristics of CuO thin films. Nevertheless, they prepared CuO thin films via magnetron sputtering. Varghese et al. [26], also studied the PL emission of sol-gel prepared CuO thin film. The main aim of their study was to investigate the effect of CuO on the photoluminescence quenching and photocatalytic activity of ZnO multilayered thin films. They prepared and studied PL spectra of just one CuO thin film. Most recently, Modhi et al. [27], compared the PL spectra of CuO and CuO-CeO$_2$ nanocomposite thin films prepared via spray deposition.

Accordingly, in the present study, the spray pyrolysis technique was adopted to deposit CuO thin films at different substrate temperatures. The optical constants, including absorption coefficient, band gap, Urbach energy, refractive index, extinction coefficient, and real and imaginary parts of

the dielectric constant were computed using experimental transmittance and reflectance data. The resulting CuO thin films were also excited by a 485 nm wavelength and the recorded PL spectra were investigated.

2. Experimental details

2.1 Thin film deposition

To deposit CuO thin films, first, soda-lime glass was ultrasonicated in hydrochloric acid, acetone, and deionized water, respectively, and dried with filtered air. Then, the precursor solution was prepared by adding 0.256 gr copper chloride dihydrate (CuCl$_2$.2H$_2$O) to 30 mL deionized and stirring for 30 min. The resulting solution was spray-deposited via a homemade spray apparatus with a custom glass gun (0.2 mm nozzle diameter) and the spray condition of 0.9 bar carrier gas (compressed filter air), 292 cm nozzle-substrate distance, 2 mL/min solution flow rate and substrate temperature of $450-550°$ C with 25° C steps.

2.2 Instrumentation and characterization

To investigate the structural properties, the X-ray diffraction (XRD) pattern of the spray-deposited CuO thin films was recorded by X'Pert PRO PANalytical diffractometer with Cu-Kα radiation and 0.026 scan steps. Moreover, a
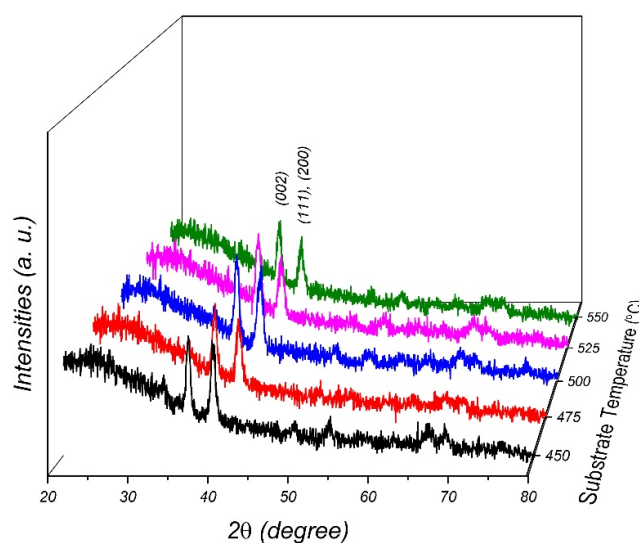
Figure 1. XRD pattern of the spray-deposited CuO thin films at different substrate temperatures.
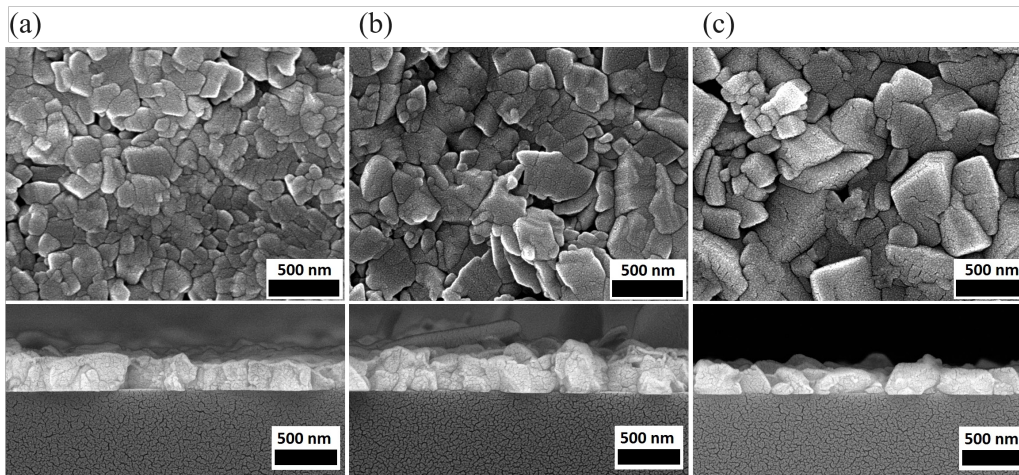
Figure 2. Surface and cross-section FESEM image of the spray-deposited CuO thin films at a) 450 °C, b) 500 °C, c) f 550 °C.

MIRA3TESCAN-XMU field-emission scanning electron microscope (FESEM) was utilized to study the surface morphology, measure the thickness, and record the energy-dispersive X-ray spectroscopy (EDX) of the prepared CuO thin films at different substrate temperatures. To study the optical properties, the transmittance and reflectance spectra of the resulting CuO thin films were monitored by a Perkin-Elmer Lambda 25 spectrophotometer. Finally, a Perkin-Elmer Ls55 fluorescence spectrometer was utilized to study the PL spectra of the spray-deposited CuO thin films.

3. Results and discussion

3.1 Structural properties

The recorded XRD pattern of the CuO thin films spray-deposited at different substrate temperatures is presented in Fig. 1 along with CuO JCPDS card No. 045-0937. The patterns depict two prominent peaks around 36° and 39° corresponding to (002) and (111) planes, indicative of the CuO monoclinic crystal structure (JCPDS card No. 045-0937) [28]. Besides, there are peaks with rather small intensities which are also well-matched with the JCPDS card. The small intensity in the aforementioned peaks might be due to the low level of crystallinity in CuO, as well as the fairly low thickness of the prepared CuO thin films (Table 1).

To study the intensity variation, the texture coefficient (TC) was calculated for the prominent peaks via the following equation:

$$TC(hkl) = \frac{I(hkl)/I_0(hkl)}{\frac{1}{N}\sum_N I(hkl)/I_0(hkl)} \qquad (1)$$

where I is the measured intensity of the (hkl) plane, I_0 is the standard intensity of the (hkl) plane from the JCPDS file, and N is the number of diffraction peaks [29]. The results along with the other structural parameters are presented in Table 1. As can be seen, up to 500° C, the TC for both (002) and (111) planes increase with substrate temperature and decreases with further substrate temperature rise. The

variation in the texture coefficient might be partially related to the thickness of the CuO thin films.

As presented in Table 1, the thickness variation follows the same trend with increasing the substrate temperature. Moreover, there is no significant difference between the values of TC for both dominant planes in each prepared CuO thin film. Up to 500° C, TC (111) is slightly larger than TC (002), and after that, the TC (002) slightly exceeds TC (111).

The lattice constant ($a \neq b \neq c$, $\alpha = \gamma = 90° \neq \beta$) and unit cell volume ($V$) of the monoclinic CuO crystal structure were calculated by the following equations:

$$\frac{1}{d^2} = \frac{1}{\sin^2\beta}\left(\frac{h^2}{a^2} + \frac{k^2\sin^2\beta}{b^2} + \frac{l^2}{c^2} - \frac{2hl\cos\beta}{ac}\right) \qquad (2)$$

$$V = abc\sin\beta \qquad (3)$$

where (hkl) are the Miller indices and d is the interplanar distance [30, 31].

For further structural examination, the crystallite size of the prepared CuO thin films was estimated using Scherrer's equation for the mentioned two prominent peaks [32, 33]. As presented in Table 1, the crystallite size slightly decreases with increasing the substrate temperature. It seems that the substrate temperature of 450° C provided the optimum condition for CuO crystallite growth. Note that the FWHM is the result of both crystallite size and strain in the crystal structure, and Scherrer's equation does not consider the contribution of strain in the FWHM. Using more sophisticated methods such as the Williamson-Hall method, one can estimate both the crystallite size and strain simultaneously; however, the accuracy of these methods depends on the number of peaks in the XRD patterns [34, 35]. In this study, due to the fairly low thickness of the deposited CuO thin films (Table 1) as well as the low level of crystallinity of CuO, the number of distinctive peaks which can be used in the Williamson-Hall method is not sufficient.

3.2 Morphological properties

The systematic variation of the surface morphology of the CuO thin films spray-deposited at 450, 500, and 550° C,
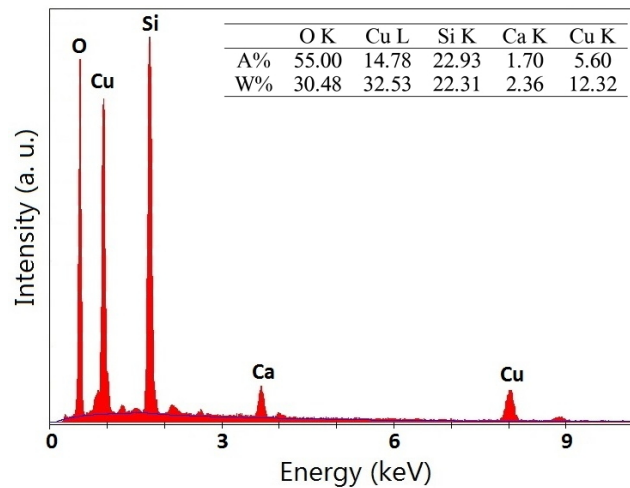
Figure 3. EDX spectrum of the CuO thin film spray-deposited at 500 °C.

along with the cross-section micrographs of the mentioned films, are represented in Fig. 2.

The surface morphology of the prepared films exhibits regular grains with distinguishable boundaries. Compared to the other thin films, the grains on the surface of the spray-deposited thin films at 450° C are denser with a wider grain size distribution. As the substrate temperature rises, the grain size dramatically increases, to the extent that the grain sizes at 550° C are several times larger than the ones for 450° C. A variation in the morphology of CuO thin films can be observed in the cross-section images of the spray-deposited CuO thin films. The compactness and homogeneity of the film grown at 450° C are also noticeable in the cross-section image. Based on the cross-section image of the CuO thin films resulting from the 550° C substrate temperature, the grain size in some cases is even larger than the film thickness. According to the cross-section images, all the prepared CuO films are fairly thin (< 310 nm). The thickness first slightly increases with temperature from 265 nm for 450° C to 310 nm for 500° C , and decreases to 230

nm for 550° C. It seems that the substrate temperature of 500° C, along with the other spray parameters, provides the optimum condition for CuO thin film growth. The decrease with the temperature rise beyond 500° C might be due to spray solution evaporation through the deposition chamber and splashing from the substrate surface.

Moreover, the recorded EDX analysis of the CuO thin film spray-deposited at 500° C (Fig. 3) detected Cu, O, and glass elements (Si, O, and Ca). The fairly low thickness of the CuO thin film can be a compelling explanation for the abundance of O and the existence of Si and Ca.

3.3 Optical properties

The recorded experimental transmittance and specular reflectance data for the prepared CuO thin films, in the wavelength region of 300 to 1100 nm, are represented in Fig. 4. As expected, the transmittance pattern is well-matched with the proper absorber layer characteristics. Accordingly, there is a considerable absorption in the visible region ($400 - 750$ nm) for the CuO thin films, which gradually de-
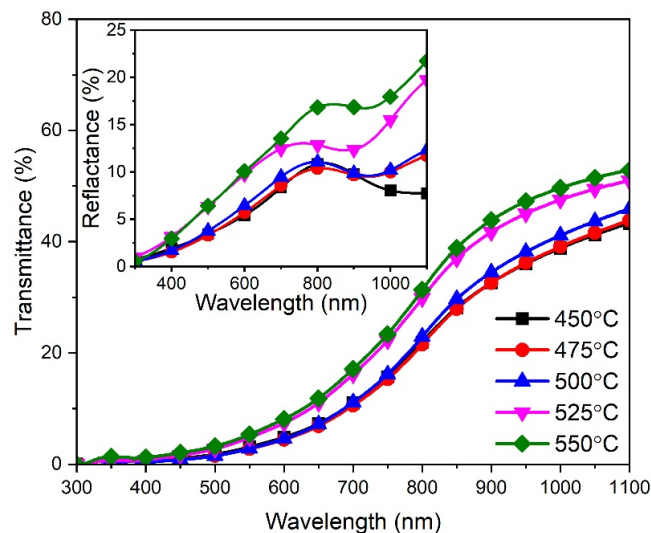

Figure 4. Optical transmittance spectra of the resulting CuO thin films grown at different substrate temperatures; inset shows optical reflectance spectra of the prepared CuO thin films.
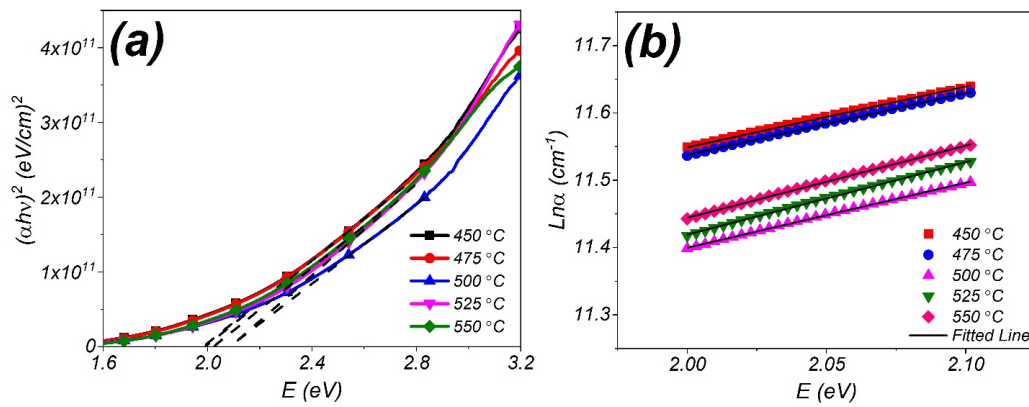
Figure 5. a) Plots of $(\alpha h\nu)^2$ vs. hν for the optical band gap estimation; b) plots of Lnα as a function of photon energy for Urbach energy estimation.

creases in the infrared region (750 − 1100 nm) [36]. There is no significant difference in the transmittance of the CuO thin films deposited at 450, 475, and 500° C. However, it slightly increases for the films deposited at 525 and 550° C.

3.3.1 Band gap and Urbach energy

To estimate the band gap of the spray-deposited CuO thin films at different substrate temperatures, the absorption coefficient (α) was first calculated using the measured thickness (t), recorded transmittance (T), reflectance (R), and the following formula [37]:

$$\alpha = \frac{1}{t} \ln\left[\frac{(1-R^2)}{2T} + \sqrt{\frac{(1-R)^4}{4T^2} + R^2} \right] \qquad (4)$$

Subsequently, the direct band gap of the resulting CuO films was estimated by plotting $(\alpha h\nu)^2$ vs. $h\nu$, known as Tauc plot, and extrapolating the linear part of the plot to $(\alpha h\nu)^2 = 0$ (Fig 5a) [38]. The results are also presented in Table 2. There is a slight reduction in the resulting band gaps with the substrate temperature. According to the quantum confinement effect, as the crystallite size decreases, a band gap increase can be expected [39, 40]. As discussed earlier, the crystallite size of the prepared CuO thin films slightly declines with the substrate temperature, which is consistent with the band gap variation. Note that depending on the deposition technique and parameters, a wide range

of band gap energies (1.3 − 2.1 eV) has been reported for CuO thin films. The estimated band gap values in this study (~ 2.00 eV) demonstrate good agreement with the reported values for the spray-deposited CuO thin films in the literature [41–43].

Following the lattice disorder in the poor crystalline materials which is the case for the CuO structure, the density of electron states develops tails into the band gap and causes band gap reduction [44]. The mention tail is called Urbach energy (E_U), shown by the following equation:

$$\alpha = \alpha_0 \exp\left(\frac{h\nu}{E_u} \right) \qquad (5)$$

where α_0 is a constant. Accordingly, the Urbach energy can be estimated by plotting $\ln(\alpha)$ vs. $h\nu$ and the calculated inverse slope of the $\ln(\alpha)$ near the band gap (Fig. 5b) [45]. The results are listed in Table 2. There is a slight reduction in the value of E_U with substrate temperature, which is consistent with the band gap variation. Furthermore, the structural defects and disorders in the prepared thin films decline with increasing the substrate temperature.

3.3.2 Reflective index and extinction coefficient

To gain detailed insight into the interaction between a material and incident light, it is necessary to compute and study the variation of refractive index and extinction coefficient.
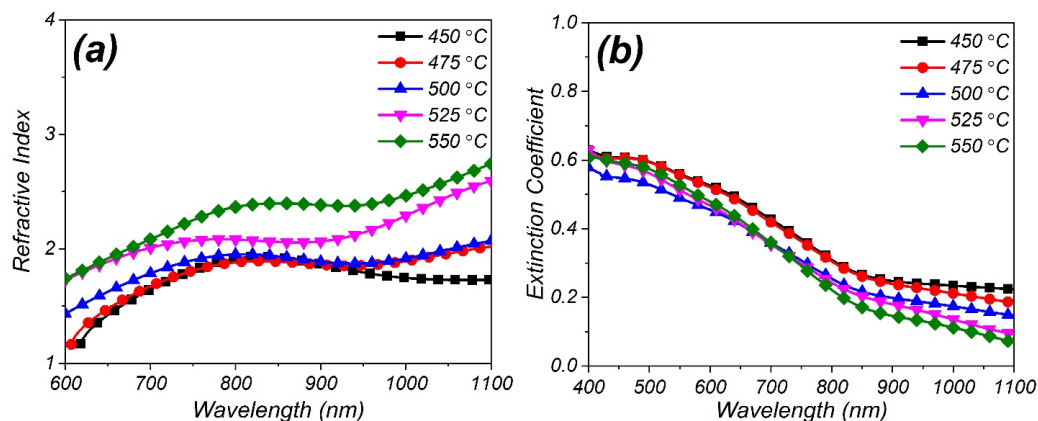

Figure 6. Variation of a refractive index and b extinction coefficient of the spray-deposited CuO thin films.

Table 2. Estimated band gap and Urbach energy of the prepared CuO thin films.

Substrate Temperature	Band gap	Urbach Energy
T (° C)	E_g (eV)	E_U (eV)
450	1.98	1.11
475	1.99	1.09
500	2.08	1.04
525	2.09	0.93
550	2.02	0.93

The aforementioned parameters are dimensionless numbers generally associated with refraction and absorption of light in a material, respectively [46].

The extinction coefficient (k) is basically proportionate to the absorption coefficient (α) and can, therefore, be calculated for any wavelength (λ) using the following equation [47]:

$$k = \frac{\alpha\lambda}{4\pi} \qquad (6)$$

Besides, the refractive index (n) of the resulting CuO thin films was calculated using experimental reflectance data (R), extinction coefficient (k), and the following equation [48]:

$$n = \frac{(1+R)}{(1-R)} + \sqrt{\frac{4R}{(1-R)^2} - k^2} \qquad (7)$$

The results of the refractive index and extinction coefficient for the spray-deposited CuO thin films are represented in Fig. 6. As the deposition temperature increases, the refractive index rises, but the extinction coefficient slightly decreases. Furthermore, for all the resulting CuO thin films, the extinction coefficient is reduced at a higher wavelength (lower energy).

3.3.3 Dielectric constants

The complex dielectric constant consisting of real (ε_1) and imaginary (ε_2) components can be computed using the calculated refractive index (n), extinction coefficient (k), and

the following expressions [49]:

$$\varepsilon_1 = n^2 - k^2 \qquad (8)$$

$$\varepsilon_2 = 2nk \qquad (9)$$

The photon energy dependence of ε_1 and ε_2 was calculated and depicted in Fig. 7a and b, respectively. The real (ε_1) and imaginary (ε_2) parts of the dielectric constant are known to represent dispersion (storage) and dissipation (loss) of energy while light propagates through a material, respectively [50]. Apart from the CuO thin film deposited at 450° C, for the other CuO thin films, the real part of the dielectric constant, ε_1, exhibits a constant increase with raising the wavelength, with a shoulder peak around 800 nm. Moreover, the substrate temperature dependence of the ε_1 is found to be proportional; thus, the largest value of the ε_1 belongs to the CuO thin films spray-deposited at 550° C. On the contrary, for all the prepared CuO films, ε_2 decreases with the substrate temperature elevation, and the general variation with the wavelength is decreasing.

The dissipation factor or tan δ refers to the loss-rate of energy of light in material and can be calculated by dividing ε_2 by ε_1 [51]:

$$\tan\delta = \frac{\varepsilon_2}{\varepsilon_1} \qquad (10)$$

Fig. 8 depicts the resulting dissipation factor for the prepared CuO thin films at different substrate temperatures. The dissipation factor decreases with increasing the wavelength. Furthermore, increasing the deposition temperature
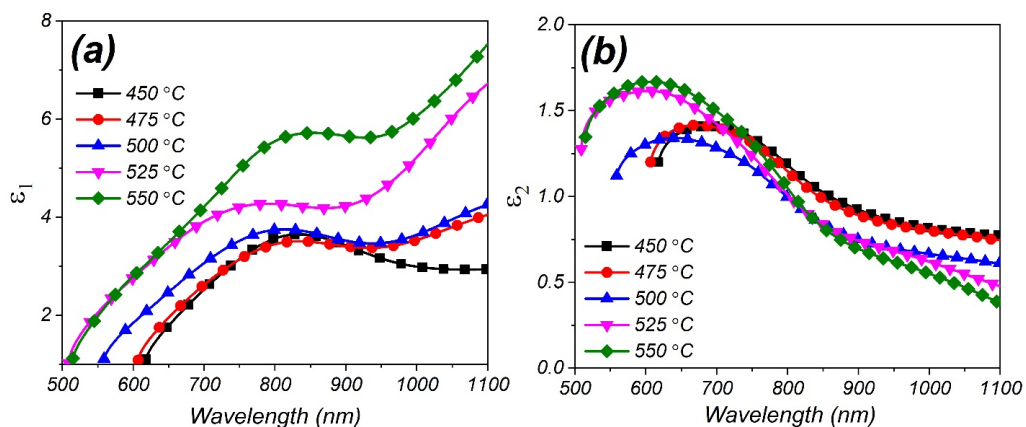

Figure 7. Variation of a) real and b) imaginary parts of the dielectric constant of the CuO thin films prepared at different substrate temperatures.
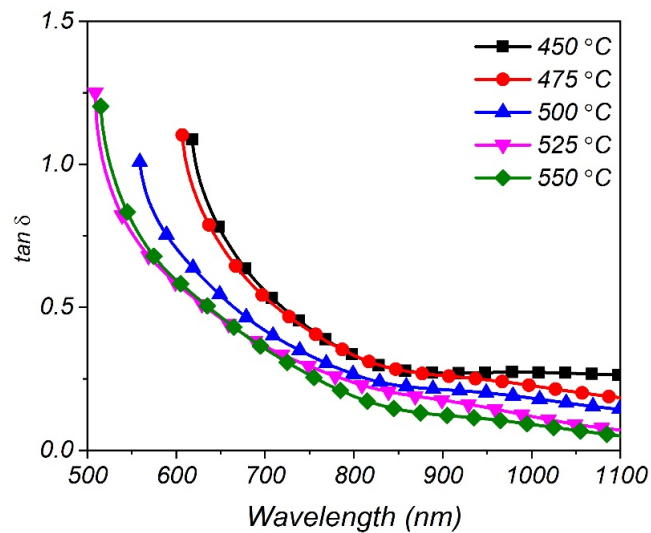
Figure 8. Variation of dissipation factor with wavelength for the prepared CuO thin films.

decreases the dissipation factor. The smaller the dissipation factor is, the more storage energy occurs; thus, a higher deposition temperature is in favor of energy storage in the spray-deposited CuO thin films.

3.3.4 Photoluminescence properties

PL is a common analysis to investigate the electronic state of a material, in which the excited target material absorbs a photon and excites an electron to higher states. The recorded radiation resulting from the excited electron returning to a lower energy state provides beneficial information about the electronic structure of the material [52]. The room-temperature PL spectra of the spray-deposited CuO thin films excited at 486 nm were recorded in the wavelength range of 200 to 800 nm (Fig. 9).

As a result of the 486 nm excitation wavelength, all the prepared CuO thin films showed almost the same vivid PL peaks around 505 nm (2.46 eV), 547 nm (2.27 eV), 630 nm (1.97 eV), and three shoulder peaks around 520 nm (2.38 eV), 590 nm (2.10 eV), and 650 nm (1.91 eV). Since the effective mass of the electron and hole shows considerable variations in CuO, it is hard to find the precise source of the recorded PL emissions in the spectra [53]. The 630 nm emission is fairly close to the estimated band gap of the prepared film, suggesting that the 630 nm emission might correspond to the near-band-edge emission. Both the 505 nm and 520 nm are fairly close to the energies reported to
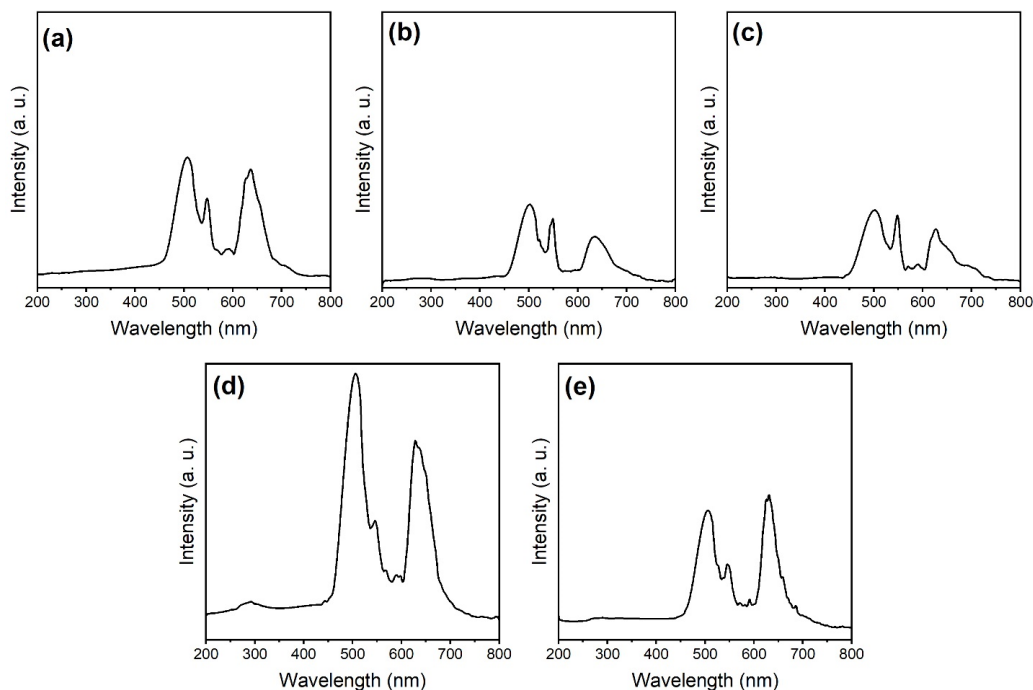

Figure 9. PL spectra of the CuO thin films spray-deposited at a) 450 °C, b) 475 °C, c) 500 °C, d) 525 °C, e) 550 °C and excitation wavelength of 485 nm.

be the results of singly ionized oxygen vacancies [25, 53]. The 547 nm and 590 nm are assigned to the excitonic transitions from sublevels of the conduction band to the valence band [25]. It is reported that the presence of the other oxidation state of copper is responsible for PL peak emissions between 635 to 670 nm [54, 55]. Therefore, the 650 nm emission might be due to the presence of the other phase of copper oxide. Based on Fig. 9, the intensity of the 650 nm peak first decreases with the deposition temperature elevation up to 500° C, and then rises at the higher deposition temperatures. At 500° C, the peak intensities related to the ionized oxygen vacancies are at a minimum, implying the CuO thin film growth with fewer defects. As mentioned earlier, the substrate temperature of 500° C seems to provide the best condition for the growth of the CuO thin film, which can be a good explanation for the lower intensity of the recorded PL peaks.

4. Conclusion

CuO thin films, with a thickness range of 230 to 310 nm, were grown at different substrate temperatures, and the structural, morphological, optical, and PL characteristics were investigated. Scherrer's equation was utilized to calculate the crystallite size of the preferred orientations. Based on the results, the largest crystallite size belonged to the film deposited at 450° C and gradually declined with increasing the substrate temperature. Accordingly, the 450° C seems to be the optimum condition for crystallite growth. Nevertheless, based on the FESEM images of the prepared films, the grain size increased with substrate temperature to the extent that it was comparable with the thickness of the CuO thin film deposited at 550° C. The estimated ($\sim$ 2.00 eV) band gap was quite close to the optimum band gap value of a desirable absorber layer. The recorded transmittance and reflectance were utilized to compute the optical constant of the prepared CuO thin films. The results revealed that as the substrate temperature rises, the extinction coefficient slightly decreases while the refractive index increases. The real (ε_1) and imaginary (ε_2) parts of the dielectric constant exhibited increments and decrements, respectively. The recorded PL spectra resulting from the 485 nm excitation wavelength exhibited three main and three shoulder peaks. The intensity variation of the PL peaks indicated that the CuO thin film grown at the 500° C substrate temperature has less ionized oxygen vacancies and impurities induced by the presence of other phases of copper oxide. Generally, the results provide accurate information about the physical and optical properties of the spray-deposited CuO thin film, demonstrating the adequacy of CuO thin films as an absorber layer in optoelectronic devices.

Ethical approval
This manuscript does not report on or involve the use of any animal or human data or tissue. So the ethical approval is not applicable.

Conflict of Interests
The author declare that they have no known competing financial interests or personal relationships that could have appeared to influence the work reported in this paper.

References

[1] H. Anousha. "Properties of nanoscale copper oxide thin film deposited by plasma focus device.". *Journal of Theoretical and Applied Physics*, **16**:1–10, 2022. DOI: https://doi.org/10.30495/jtap.162245.

[2] T. V. Anitha, K. Gadha Menon, K. Venugopal, and T. V. Vimalkumar. "Investigating the role of film thickness on the physical properties of sol-gel coated CuO thin films: Discussing its potentiality in optoelectronic applications.". *Materials Science and Engineering: B*, **299**:116960, 2024. DOI: https://doi.org/10.1016/j.mseb.2023.116960.

[3] A. Abdel-Galil and N. L. Moussa. "Nanostructure CuO thin film deposited by spray pyrolysis for technological applications.". *Radiation*

Physics and Chemistry, **212**:111119, 2023. DOI: https://doi.org/10.1016/j.radphyschem.2023.111119.

[4] A. Roy and A. Majumdar. "Optimization of CuO/CdTe/CdS/TiO$_2$ solar cell efficiency: A numerical simulation modeling.". *Optik*, **251**:168456, 2021. DOI: https://doi.org/10.1016/j.ijleo.2021.168456.

[5] H. Z. Asl and S. M. Rozati. "Some physical properties of n-IZO/p-CuO thin film heterojunction diodes completely made by spray pyrolysis.". *Journal of Materials Science: Materials in Electronics*, **29**:4365–4372, 2018. DOI: https://doi.org/10.1007/s10854-017-8385-1.

[6] R. Ma, R. Pathak, D. Zheng, Y. Zhang, J. Xing, J. Liu, Y. Jiang, M. Xiao, and F. Wu. "Preparation and photoelectrochemical properties of hierarchical heterostructure ZnO/CuO array.". *Applied Physics A*, **127**:100, 2021. DOI: https://doi.org/10.1007/s00339-020-04242-6.

[7] H. A. Al-Jawhari. "A review of recent advances in transparent p-type Cu$_2$O-based thin film transistors.". *Materials Science in Semiconductor Processing*, **40**:241–252, 2015. DOI: https://doi.org/10.1016/j.mssp.2015.06.063.

[8] M. E. Güldüren, D. İskenderoğlu, H. Güney, E. Gür, M. Acar, and S. Morkoç Karadeniz. " Investigating the influence of Ni doping on the CuO thin films deposited via ultrasonic spray pyrolysis: Structural, optical and H$_2$ gas sensing analyses.". *International Journal of Hydrogen Energy*, **48**:828–839, 2023. DOI: https://doi.org/10.1016/j.ijhydene.2022.09.283.

[9] Y. Yang, J. Li, Y. Jiang, B. Wang, Y. Zhang, T. Wang, X. Xiong, and Y. Wang. "Thermal oxidation and SILAR method to prepare CuO/CdS composite nanostructure and its enhanced photocatalytic properties.". *Journal of Electronic Materials*, **50**:4762–4769, 2021. DOI: https://doi.org/10.1007/s11664-021-08977-7.

[10] B. S. Kang, S-E. Ahn, M-J. Lee, G. Stefanovich, K. H. Kim, W. X. Xianyu, C. B. Lee, Y. Park, I. G. Baek, and B. H. Park. "High-current-density CuOx/InZnOx thin-film diodes for cross-point memory applications.". *Advanced Materials*, **20**:3066–3069, 2008. DOI: https://doi.org/10.1002/adma.200702932.

[11] N. Aghilizadeh, A. H. Sari, and D. Dorranian. "Role of Ar/O$_2$ mixture on structural, compositional and optical properties of thin copper oxide films deposited by DC magnetron sputtering.". *Journal of Theoretical and Applied Physics*, **11**:1–6, 2017. DOI: https://doi.org/10.1007/s40094-017-0268-6.

[12] B. Yan, Y. Wang, T. Jiang, and X. Wu. "Synthesis and enhanced photocatalytic property of La-doped CuO nanostructures by electrodeposition method.". *Journal of Materials Science: Materials in Electronics*, **27**:5389–5394, 2016. DOI: https://doi.org/10.1007/s10854-016-4439-z.

[13] A. D. Faisal and W. K. Khalef. "Morphology and structure of CuO nanostructures grown via thermal oxidation on glass, silicon, and quartz at different oxidation temperatures.". *Journal of Materials Science: Materials in Electronics*, **28**, 2017. DOI: https://doi.org/10.1007/s10854-017-7844-z.

[14] S. Visalakshi, R. Kannan, S. Valanarasu, H-S. Kim, A. Kathalingam, and R. Chandramohan. "Effect of bath concentration on the growth and photovoltaic response of SILAR-deposited CuO thin films.". *Applied Physics A*, **120**:1105–1111, 2015. DOI: https://doi.org/10.1007/s00339-015-9285-y.

[15] L. Xu, F. Xian, and W. Kuang. "Growth of high quality CuO thin film and investigation of its abnormal luminescence behavior.". *Physica B: Condensed Matter*, **673**:415505, 2024. DOI: https://doi.org/10.1016/j.physb.2023.415505.

[16] H. Z. Asl and S. M. Rozati. "Spray deposited nanostructured CuO thin films: Influence of substrate temperature and annealing process.". *Materials Research*, **21**, 2018. DOI: https://doi.org/10.1590/1980-5373-MR-2017-0754.

[17] H. Zare Asl and S. M. Rozati. "Electrochemical performance improvement of completely spray-deposited FTO/Zn-doped Co$_3$O$_4$ double layer thin films: Influence of Zn doping.". *Chemical Physics Letters*, **815**:140364, 2023. DOI: https://doi.org/10.1016/j.cplett.2023.140364.

[18] V. Saravanan, P. Shankar, G. K. Mani, and J. B. B. Rayappan. "Growth and characterization of spray pyrolysis deposited copper oxide thin films: Influence of substrate and annealing temperatures.". *Journal of Analytical and Applied Pyrolysis*, **111**:272–277, 2015. DOI: https://doi.org/10.1016/j.jaap.2014.08.008.

[19] H. Z. Asl and S. M. Rozati. "Effects of HCl and methanol in the precursor on physical properties of spray-deposited nanostructured CuO thin films for solar applications.". *Journal of Electronic Materials*, **46**:5020–5027, 2017. DOI: https://doi.org/10.1007/s11664-017-5510-0.

[20] S. Keerthana, M. B. A. Titlin, C. R. Dhas, R. Venkatesh, and S. E. S. Monica. "Unraveling the role of solvent type in the physical and chemiresistive gas sensing properties of nebulizer-sprayed CuO films.". *Materials Science and Engineering: B*, **297**:116821, 2023. DOI: https://doi.org/10.1016/j.mseb.2023.116821.

[21] R. J. Deokate, A. V. Moholkar, G. L. Agawane, S. M. Pawar, J. H. Kim, and K. Y. Rajpure. "Studies on the effect of nozzle-to-substrate distance on the structural, electrical and optical properties of spray deposited CdIn$_2$O$_4$ thin films.". *Applied Surface Science*, **256**:3522–3530, 2010. DOI: https://doi.org/10.1016/j.apsusc.2009.12.102.

[22] M. Lamri Zeggar, L. Chabane, M. S. Aida, N. Attaf, and N. Zebbar. "Solution flow rate influence on properties of copper oxide thin films deposited by ultrasonic spray pyrolysis.". *Materials Science in Semiconductor Processing*, **30**:645–650, 2015. DOI: https://doi.org/10.1016/j.mssp.2014.09.026.

[23] I. S. Yahia, A. A. M. Farag, S. El-Faify, F. Yakuphanoglu, and A. A. Al-Ghamdi. "Synthesis, optical constants, optical dispersion parameters of CuO nanorods.". *Optik - International Journal for Light and Electron Optics*, **127**:1429–1433, 2016. DOI: https://doi.org/10.1016/j.ijleo.2015.10.021.

[24] L. Xu, G. Zheng, S. Pei, and J. Wang. "Investigation of optical bandgap variation and photoluminescence behavior in nanocrystalline CuO thin films.". *Optik*, **158**:382–390, 2018. DOI: https://doi.org/10.1016/j.ijleo.2017.12.138.

[25] C. R. Gobbiner, G. R. Dillip, S. W. Joo, and D. Kekuda. "Heterogeneity of photoluminescence properties and electronic transitions in copper oxide thin films: A thickness dependent structural and optical study.". *Ceramics International*, **44**:16984–16991, 2018. DOI: https://doi.org/10.1016/j.ceramint.2018.06.140.

[26] J. Varghese and R. Vinodkumar. "Effect of CuO on the photoluminescence quenching and photocatalytic activity of ZnO multilayered thin films prepared by sol-gel spin coating technique.". *Materials Research Express*, **6**:106405, 2019. DOI: https://doi.org/10.1088/2053-1591/ab3596.

[27] M. K. Modhi and J. M. Rzaij. "Synthesis and characterization study of CuO thin film and CuO-CeO$_2$ nanostructured composite using chemical spray pyrolysis.". *AIP Conference Proceedings*, **2591**:030066, 2023. DOI: https://doi.org/10.1063/5.0120468.

[28] H. Z. Asl and S. M. Rozati. "Spray deposition of n-type cobalt-doped CuO thin films: Influence of cobalt doping on structural, morphological, electrical, and optical properties.". *Journal of Electronic Materials*, **49**:1534–1540, 2019. DOI: https://doi.org/10.1007/s11664-019-07858-4.

[29] H. Z. Asl and S. M. Rozati. " Influence of texture coefficient on the electrical properties of spray-deposited fluorine-doped tin oxide thin film.". *Journal of Materials Science: Materials in Electronics*, **32**:1668–1676, 2021. DOI: https://doi.org/10.1007/s10854-020-04936-w.

[30] H. Z. Asl and S. M. Rozati. "Influence of structural properties on the electrochemical performance of FTO/CuO double-layer thin-film spray-deposited from different precursor solutions.". *Applied Physics A*, **129**:786, 2023. DOI: https://doi.org/10.1007/s00339-023-07070-6.

[31] A. Prakash and M. G. Mahesha. "Harnessing the tunability of intrinsic defects in isovalent Zn doped spray deposited CuO thin films.". *Materials Chemistry and Physics*, **309**:128443, 2023. DOI: https://doi.org/10.1016/j.matchemphys.2023.128443.

[32] B. D. Cullity. *"Elements of X-Ray Diffraction."*, volume . 1956.

[33] D. Nath, F. Singh, and R. Das. "X-ray diffraction analysis by Williamson-Hall, Halder-Wagner and size-strain plot methods of CdSe nanoparticles-a comparative study. ". *Materials Chemistry and Physics*, **239**:122021, 2020. DOI: https://doi.org/10.1016/j.matchemphys.2019.122021.

[34] H. Z. Asl and S. M. Rozati. "Structural, morphological, electrical, optical, and photoluminescence properties of spray-deposited ZnO thin film: effect of hydrochloric and acetic acids in the precursor.". *Journal of Materials Science: Materials in Electronics*, **31**:2537–2543, 2020. DOI: https://doi.org/10.1007/s10854-019-02790-z.

[35] V. Mote, Y. Purushotham, and B. Dole. "Williamson-Hall analysis in estimation of lattice strain in nanometer-sized ZnO particles.". *Journal of Theoretical and Applied Physics*, **6**:6, 2012. DOI: https://doi.org/10.1186/2251-7235-6-6.

[36] S. Keerthana, M. B. Arthina Titlin, C. R. Dhas, R. Venkatesh, D. Arivukarasan, and K. C. Mercy Gnana Malar. "Insights on the host precursor role play in the chemiresistive gas sensing properties of nebulizer spray-coated CuO films.". *Physica B: Condensed Matter*, **659**:414852, 2023. DOI: https://doi.org/10.1016/j.physb.2023.414852.

[37] A. R. Wassel, S. A. Mansour, F. M. Mohamed, and A. M. El-Mahalawy. "Exploration of doping-dependent structural, optical, and electrical properties of thermally evaporated CdSe thin films for improved photodetection performance.". *Journal of Alloys and Compounds*, **976**:173052, 2024. DOI: https://doi.org/10.1016/j.jallcom.2023.173052.

[38] H. Z. Asl and S. M. Rozati. "A simple route for spray deposition of ZnO thin films embedded with Ag nanoparticles: influence of Ag concentration on the structural, morphological, optical, and photoluminescence properties.". *Journal of Materials Science: Materials in Electronics*, **31**:14537–14544, 2020. DOI: https://doi.org/10.1007/s10854-020-04014-1.

[39] Y. Gupta, P. Arun, A. A. Naudi, M. V. Walz, and E. A. Albanesi. "Grain size and lattice parameter's influence on band gap of SnS thin nano-crystalline films.". *Thin Solid Films*, **612**:310–316, 2016. DOI: https://doi.org/10.1016/j.tsf.2016.05.056.

[40] N. Mohamed Basith, J. Judith Vijaya, L. John Kennedy, and M. Bououdina. "Structural, optical and room-temperature ferromagnetic properties of Fe-doped CuO nanostructures.". *Physica E: Low-dimensional Systems and*

Nanostructures, **53**:193–199, 2013. DOI: https://doi.org/10.1016/j.physe.2013.05.009.

[41] A. M. El Sayed and M. Shaban. "Structural, optical and photocatalytic properties of Fe and (Co, Fe) co-doped copper oxide spin coated films.". *Spectrochimica acta. Part A*, **149**:638–646, 2015. DOI: https://doi.org/10.1016/j.saa.2015.05.010.

[42] Y. Akaltun. "Effect of thickness on the structural and optical properties of CuO thin films grown by successive ionic layer adsorption and reaction.". *Thin Solid Films*, **594**:30–34, 2015. DOI: https://doi.org/10.1016/j.tsf.2015.10.003.

[43] F. A. Akgul, G. Akgul, N. Yildirim, H. E. Unalan, and R. Turan. "Influence of thermal annealing on microstructural, morphological, optical properties and surface electronic structure of copper oxide thin films.". *Materials Chemistry and Physics*, **147**:987–995, 2014. DOI: https://doi.org/10.1016/j.matchemphys.2014.06.047.

[44] A. S. Hassanien and A. A. Akl. "Effect of Se addition on optical and electrical properties of chalcogenide CdSSe thin films.". *Superlattices and Microstructures*, **89**:153–169, 2016. DOI: https://doi.org/10.1016/j.spmi.2015.10.044.

[45] E. K. Shokr, H. A. Mohamed, A. A. Ismail, M. F. Hasaneen, and H. M. Ali. "Optical and electrical properties of thin films of MnS/metal/MnS for photocatalysis and gas sensing applications.". **296**:171549, 2024. DOI: https://doi.org/10.1016/j.ijleo.2023.171549.

[46] A. S. Hassanien and I. Sharma. "Optical properties of quaternary a-Ge15-x Sbx Se50 Te35 thermally evaporated thin-films: refractive index dispersion and single oscillator parameters.". *Optik*, **200**:163415, 2020. DOI: https://doi.org/10.1016/j.ijleo.2019.163415.

[47] A. S. Hassanien and I. Sharma. "Synthesis, analysis, and characterization of structural and optical properties of thermally evaporated chalcogenide a-Cu-Zn-Ge-Se thin films.". *Materials Chemistry and Physics*, **311**:128524, 2024. DOI: https://doi.org/10.1016/j.matchemphys.2023.128524.

[48] I. M. El Radaf and R. M. Abdelhameed. "Surprising performance of graphene oxide/tin dioxide composite thin films.". *Journal of Alloys and Compounds*, **765**, 2018. DOI: https://doi.org/10.1016/j.jallcom.2018.06.277.

[49] M. Kamaliana, E. Hasani, L. Babazadeh Habashi, and M. Gholizadeh Arashti. "Impact of post-deposition annealing on the optical, electrical, and structural properties of CdS thin films for solar cell applications.". *Physica B: Condensed Matter*, **674**:415524, 2024. DOI: https://doi.org/10.1016/j.physb.2023.415524.

[50] H. Y. Zahran, J. Iqbal, and I. S. Yahia. "Optical constants and nonlinear calculations of fluorescein/FTO thin film optical system.". *Physica B: Condensed Matter*, **500**:98–105, 2016. DOI: https://doi.org/10.1016/j.physb.2016.07.034.

[51] E. R. Shaaban, M. Y. Hassaan, M. G. Moustafa, A. Qasem, G. A. M. Ali, and E. S. Yousef. "Optical constants, dispersion parameters and non-linearity of different thickness of As40S45Se15 thin films for optoelectronic applications.". *Optik*, **186**:275–287, 2019. DOI: https://doi.org/10.1016/j.ijleo.2019.04.097.

[52] N. Dogru, S. Gurakar, T. Serin, and A. Yildiz. "Comparative structure, optical and electrical characteristics of sol-gel-deposited In-, Ga-, and Sn-doped CuO thin films.". *Materialia*, **32**:101970, 2023. DOI: https://doi.org/10.1016/j.mtla.2023.101970.

[53] K. Sahu, A. Bisht, S. A. Khan, A. Pandey, and S. Mohapatra. "Engineering of morphological, optical, structural, photocatalytic and catalytic properties of nanostructured CuO thin films fabricated by reactive DC magnetron sputtering.". *Ceramics International*, **46**:7499–7509, 2020. DOI: https://doi.org/10.1016/j.ceramint.2019.11.248.

[54] X. Zhao, P. Wang, Z. Yan, and N. Ren. "Room temperature photoluminescence properties of CuO nanowire arrays.". *Optical Materials*, **42**:544–547, 2015. DOI: https://doi.org/10.1016/j.optmat.2014.12.032.

[55] S. Dagher, Y. Haik, A. I. Ayesh, and N. Tit. "Synthesis and optical properties of colloidal CuO nanoparticles.". *Journal of Luminescence*, **151**:149–154, 2014. DOI: https://doi.org/10.1016/j.jlumin.2014.02.015.